Synthesis and Solid-State Characterization of Amphiphilic Tail-End Pyridinium Polymethacrylates

Pascal Y. Vuillaume,[†] C. Geraldine Bazuin,*,[†] and Jean-Claude Galin[‡]

Centre de recherche en sciences et ingénierie des macromolécules (CERSIM), Département de chimie, Université Laval, Québec, Canada G1K 7P4; and Institut Charles Sadron (ICS), CNRS-ULP, 6 rue Boussingault, 67083 Strasbourg Cédex, France

ABSTRACT: The synthesis of a new series of cationic tail-end polyamphiphiles of the type, poly(ω-pyridinium alkyl methacrylate)s with various 4-substituted pyridinium bromide groups and with spacers of 8, 12, and 16 methylene units, obtained by free radical polymerization in aqueous micellar solution, is described, and the thermal and structural characteristics in the solid-state have been studied. All of the polymers show a single glass transition in the range 39−105 °C, whose value depends strongly both on the spacer length, due to internal plasticization, and on the specific nature of the pyridinium moiety, where higher T_g's can be related to greater rigidity of the pyridinium group. The polymers are all birefringent between crossed polarizers, in some cases up to their degradation temperatures. X-ray diffraction investigations indicate that they tend to self-organize into an amorphous lamellar morphology that appears to be better defined the longer the alkyl spacer and whose details depend also on the specific pyridinium moiety. Thus, it is shown that the effects of ionic interactions and of the amphiphilic character of the polymers on their thermal and structural properties are clearly modulated by the alkyl spacer length and by mesogen-related parameters such as rigidity and bulkiness.

Introduction

The solid-state properties of ionic side-chain polyamphiphiles or polysoaps—specifically, polymers having distinct hydrophilic (ionic) and hydrophobic moieties in the side-chain—have received little attention compared to their solution properties.[1,2] In the past few years, however, several reports on the bulk properties of such polyamphiphiles have appeared.[3−17] Laschewsky and co-workers,[3−7] in particular, have contributed systematic investigations involving a variety of molecular architectures where the ionic hydrophilic site is located at different positions in the amphiphilic side chain (at the ionic headgroup or at the end or near the middle of the flexible tail). The ionic groups, in their case, are principally of the zwitterionic type, both sulfobetaine and carbobetaine, with a few of the quaternary ammonium salt type. Other systems involve the simultaneous presence of ionic and thermotropic moieties in separate locations in the side chain, the ionic group generally being in the vicinity of the polymer backbone.[10,15−17]

The presence of a flexible moiety might be expected to lead to materials with accessible glass transition temperatures (by contrast with conventional polyelectrolytes in the solid state),[18] and the amphiphilic character of the materials might favor supramolecular morphologies. These tendencies have indeed been observed in many of the polyamphiphiles studied, with details apparently dependent on various molecular characteristics, which are still poorly understood. A glass transition, for example, although detected in a number of cases,[6,7,9−12] is not always apparent,[3,6] and its dependence on specific molecular parameters remains obscure.

Given the paucity of systematic studies on these materials in the bulk, we wished to focus on cationic polyamphiphiles of the tail-end type—that is, where the ionic group is located at or near the extremity of the side-chain, far from the polymer backbone—and investigate the effects of varying both the spacer length and the nature of the cationic moiety on the thermal and structural properties. Thus, we describe herein the synthesis and solid-state properties of the polymers listed in Table 1, all based on a polymethacrylate backbone. The choice of cationic moieties was inspired, in part, by our previous studies of some low molar mass liquid crystalline analogues in the bulk.[19−21] Several of these are clearly reminiscent of ionic versions of classical (albeit short) thermotropic mesogens.

The acronyms listed in Table 1 identify successively the polymer backbone (PM for polymethacrylate, M indicating the corresponding monomer), the number n of methylene carbons in the side chain spacer (Cn), and the specific terminal 4-substituted pyridinium bromide moiety Y (MP, CP, DMAP, TP, and PP for 4-methylpyridinium, 4-cyanopyridinium, 4-dimethylaminopyridinium, 4-tolylpyridinium, and 4-pyridylpyridinium bromide, respectively). As an example, M-C12-CP stands for 12-methacryloyloxydodecyl-4-cyanopyridinium bromide, whereas preceding this by the letter P identifies the corresponding polymer, PM-C12-CP. Only the 4-methylpyridinium derivative was synthesized with different spacer lengths ($n = 8, 12, 16$); the others were synthesized with a C12 spacer only. To ensure 100% quaternization in the polymers, they were synthesized directly by free radical polymerization of the appropriate alkylpyridinium monomers.
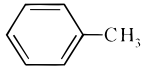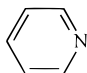
Experimental Section

Materials. Unless otherwise specified, the reagents were obtained from Aldrich. All solvents used were analytical grade. Dimethylformamide (DMF), 4-methylpyridine (4-picoline), toluene, and triethylamine were distilled over calcium hydride.

* To whom correspondence should be addressed.
† Université Laval.
‡ Institut Charles Sadron.

Table 1. Chemical Structures and Nomenclature of the Polyamphiphiles Studied

n	R	Acronym
8	CH₃	**PM-C8-MP**
12	CH₃	**PM-C12-MP**
16	CH₃	**PM-C16-MP**
12	N(CH₃)₂	**PM-C12-DMAP**
12	C≡N	**PM-C12-CP**
12	⬡–CH₃	**PM-C12-TP**
12	⬡N	**PM-C12-PP**

Acetonitrile was dried over molecular sieves (4 Å). Chloroform, ethyl acetate, 1,16-hexadecanediol, cesium carbonate (Acros and Aldrich), 4-(dimethylamino)pyridine, 4-cyanopyridine, 4,4′-dipyridine, sodium iodide (NaI), tetrabutylammonium bromide, 2-mercaptoethanol (ME), 3,5-dinitrobenzene (inhibitor) (DNB), hydroquinone (HQ), 1,12-dibromododecane, and 1,8-dibromooctane, all of the best reagent grade available, were used as received. 4-Tolylpyridine was synthesized previously in connection with another project.[21] The sodium salt of 4,4′-azobiscyanovaleric acid (ACVA) was obtained by freeze-drying from an aqueous solution of recrystallized ACVA after stoichiometric neutralization by NaOH. Column chromatography was performed using silica gel [Merck, Kieselgel 60 (70−230 mesh)], and thin-layer chromatography (TLC) was carried out on precoated silica gel plates (Merck, F-254). Water used for dialysis was purified by a Milli Q water purification system (resistance 18 MΩ).

Techniques. NMR spectra were recorded at ambient temperature with 200 or 300 MHz Bruker spectrometers. Chemical shifts, δ, are given in ppm with respect to the solvent residual resonances fixed at 7.27, 2.49, and 3.30−4.78 ppm for CDCl₃, (CD₃)₂SO, and moist CD₃OD, respectively. Infrared spectra of samples ground in KBr pellets were recorded on a Mattson FTIR spectrometer. Elemental analysis was performed in-house (ICS) and at the University of Montreal.

Thermogravimetric analysis was carried out under constant nitrogen flow (200 mL·min⁻¹) at a heating rate of 5 °C/min using a Mettler TA 3000 TGA. The samples were previously dried in vacuo at 60 °C and then in situ at 80 °C for 10 min just prior to the heating scans. The temperature of thermal degradation (T_d) was measured at the point of 5% weight loss relative to the weight at 80 °C.

Differential scanning calorimetry (DSC) was performed using a Perkin-Elmer DSC-7 calorimeter, calibrated with indium. The sample chamber was flushed with He gas at a flow rate of 40 mL/min. Measurements were performed on samples of 3 to 15 mg (less for monomers, more for polymers) sealed in aluminum pans. The monomer samples were previously dried at 40 °C in vacuo overnight, and scanned at 10 °C/min (unless otherwise specified). Transition temperatures are given by the peak maxima or minima. In cases where the DSC results are characterized by more than one transition, the melting temperature is given by that at which the virgin sample becomes transparent on heating according to nonpolarized light microscopy observations.

The polymer samples were scanned at 20 °C/min on heating, up to temperatures that did not exceed 110 °C for PM-C12-CP and 170 °C for the other polymers (unless otherwise specified). Glass transition temperatures (T_g) are given as the midpoint of the heat capacity jump. The scans were reproducible after the initial heating scan, and were independent of the prior cooling rate (20 °C/min vs nominally 200 °C/min). In view of the notorious hygroscopicity of ion-containing polymers,[18] it was verified that the drying conditions were adequate, by comparing those dried for at least 4 days at 60 °C in vacuo with those placed in pans with previously pierced covers and dried for 2 days in vacuo at 90 °C for PM-C12-CP and at 120 °C for the others; the differences observed were minimal (at most 3 °C). An additional test of a sample placed in the DSC sample chamber under N₂ at 90 °C for 16 h (thereby precluding any possible water absorption during sample transfer) also resulted in no change in T_g.

Polarizing optical microscopy (POM) observations of the samples were made using a Zeiss Axioskop equipped with a 25X Leica objective. The temperature was regulated using a Mettler FP5 temperature controller and a Mettler FP52 hot stage.

X-ray diffraction analysis was carried out with nickel-filtered Cu Kα radiation ($\lambda = 0.1542$ nm) produced by a Rigaku rotating anode X-ray generator (Rotaflex RU-200BH) operated at 55 kV and 190 mA. Collimation was effected with a Soller slit and a 1 mm pinhole. Temperature was controlled by a homemade water-cooled copper block oven. The diffraction patterns, for 2θ angles varying between 1 and 40°, were detected by a scintillation counter (SC-30) coupled to a pulse-height analyzer. Samples were placed in sealed Lindemann capillaries (Charles Supper Company) of 1.5 mm inner diameter. In general, the samples were dried in vacuo at 60 °C for 4 days, but for comparison, some were dried in vacuo at 100 °C for 3 days in an open capillary, which, after slow cooling *in vacuo,* was sealed immediately and analyzed; the overall patterns for the two drying conditions were identical, with only slight shifts of the small-angle diffraction peaks to higher angles (see Table 6), which can be associated with the loss of residual H₂O. The *d* spacing was determined from the maximum of the low-angle diffraction peaks in the smoothed diffractograms, using Bragg's relation

$$d = \lambda/(2 \sin \theta) \qquad (1)$$

The calculated lengths (l_C) of a hypothetical single-layer period were estimated using Hyperchem 3 (Hypercube Inc.) for the lowest energy conformation of the side chain with all-trans methylene units. This length corresponds to the distance between the outermost hydrogen of the methyl group on the polymer backbone to the terminal atom of the side chain, including van der Waals' radii at the extremities.

Synthesis of Monomers. Monomer Precursors. Cesium Methacrylate. In accordance with literature procedures,[22] 5.5 g (17 mmol) of Cs₂CO₃ was dissolved in 20 mL of water, to which 4.3 g (50 mmol) of methacrylic acid was then added dropwise over a period of 30 min. The solution was stirred at room temperature for 2 h and then washed three times with ether. The pure product was recovered by freeze-drying from aqueous solution, further dried at room temperature in vacuo, and then stored over P₂O₅. Yield: 2.7 g (72%) in the form of a hygroscopic white powder. Anal. Calcd for C₄H₅O₂Cs: C, 22.04, H, 2.31. Found: C, 22.03; H, 2.34. ¹H NMR (200 MHz, (CD₃)₂SO): $\delta = 5.68$ [s, 1H, CH=C cis], 5.19 [s, 1H, CH=C trans], 1.80 [s, 3H, C=C(CH₃)].

1,16−Dibromohexadecane. To a solution of 3.6 g (14 mmol) of 1,16-hexadecanediol in 50 mL of chloroform at 60 °C was added dropwise 5.07 g (19 mmol) of phosphorus tribromide. The solution was refluxed for 48 h. The organic phase was washed with water (50 mL) and then neutralized with a sodium carbonate solution, leading to an emulsion. Chloroform and water were removed by rotary evaporation. The residue was dissolved in acetone, and the precipitated sodium salts were eliminated by filtration. After concentration of the solution by rotary evaporation, the crude product was recovered by precipitation in water and filtration. Purification was performed by column chromatography [eluent: hexane/ethyl

Table 2. Melting Points of the Quaternized Monomers

monomer	melting point/°C
M-C16-MP	*a*
M-C12-MP	60[b]
M-C8-MP	paste
M-C12-CP	83[c]
M-C12-DMAP	56[c]
M-C12-TP	102[b]
M-C12-PP	96[b]

[a] Not measured. [b] Measured by DSC. [c] Measured using a non-polarized microscope (see text for more complex DSC data).

acetate (97/3 v/v)] until TLC showed complete removal of 1,16-hexadecanediol and 16-bromohexadecanol. Yield: 3.1 g (58%) in the form of a white crystalline solid. Melting point: 55 °C (DSC, 5 °C/min); lit. 56 °C.[23] Anal. Calcd for $C_{16}H_{32}Br_2$: C, 50.02; H, 8.39; Br, 41.59. Found: C, 50.12; H, 8.43; Br, 41.30. ^{1}H NMR (200 MHz, CDCl$_3$): δ = 3.44 [t, 2H, CH$_2$—Br], 1.86 [m, 2H, CH$_2$—C—Br], 1.6–1.1 [m, 28H, C—(CH$_2$)$_{14}$—C].

16-Bromohexadecyl Methacrylate (M-C16-Br). First, 2.02 g (5.2 mmol) of 1,16-dibromohexadecane was dissolved in 60 mL of DMF at 50 °C. The solution was cooled to 32 °C, 0.57 g (2.6 mmol) of cesium methacrylate and a few milligrams of hydroquinone were added, and the reaction medium was stirred for 48 h at 32 °C under argon atmosphere. The DMF was then removed by rotary evaporation, and the residue was fractionated by column chromatography [eluent: hexane/ethyl acetate (97/3 v/v)]. Unreacted 1,16-dibromohexadecane was eluted first and recovered for reuse in another synthesis. The pure monomer was then recovered, and dried in vacuo at 40 °C. Yield: 0.81 g (80%) in the form of a white waxy solid. Anal. Calcd for $C_{20}H_{37}O_2Br$: C, 61.69; H, 9.58; Br, 20.52. Found: C, 61.65; H, 9.72; Br, 20.67. ^{1}H NMR (200 MHz, CDCl$_3$): δ = 6.12 [s, 1H, CH=C—COO cis], 5.57 [s, 1H, CH=C—COO trans], 4.16 [t, 2H, CH$_2$—O], 3.44 [t, 2H, CH$_2$—Br], 1.94 [s, 3H, C=C(CH$_3$)], 1.85 [m, 2H, CH$_2$—C—Br], 1.66 [m, 2H, —CH$_2$—C—O], 1.5–1.1 [m, 24H, C—(CH$_2$)$_{12}$—C].

12-Bromododecyl Methacrylate (M-C12-Br). The same procedure was used as for M-C16-Br, but starting with 6.17 g (18.50 mmol) of 1,12-dibromododecane dissolved in 20 mL of DMF and 1.39 g (6.38 mmol) of cesium methacrylate and working at room temperature. Yield: 1.69 g (79%) in the form of a yellow oil. Anal. Calcd for $C_{16}H_{29}O_2Br$: C, 57.66; H, 8.77; O, 9.60; Br, 23.97. Found: C, 57.63; H, 8.84; O, 9.37; Br, 22.90. ^{1}H NMR (200 MHz, CDCl$_3$): δ = 6.09 [s, 1H, CH=C—COO cis], 5.54 [s, 1H, CH=C—COO trans], 4.13 [t, 2H, CH$_2$—O], 3.40 [t, 2H, CH$_2$—Br], 1.94 [s, 3H, C=C(CH$_3$)], 1.85 [m, 2H, CH$_2$—C—Br], 1.66 [m, 2H, CH$_2$—C—O], 1.5–1.1 [m, 16H, C—(CH$_2$)$_8$—C].

8-Bromooctyl Methacrylate (M-C8-Br). The same procedure was used as for M-C12-Br, starting from 2.00 g (7.34 mmol) of 1,8-dibromooctane dissolved in 25 mL of DMF and 0.8 g (3.67 mmol) of cesium methacrylate. Yield: 0.79 g (77%) in the form of a yellow oil. ^{1}H NMR (300 MHz, CDCl$_3$): δ = 6.10 [s, 1H, CH=C—COO cis], 5.56 [s, 1H, CH=C—COO trans], 4.14 [t, 2H, CH$_2$—O], 3.41 [t, 2H, CH$_2$—Br], 1.96 [s, 3H, C=C(CH$_3$)], 1.86 [m, 2H, CH$_2$—C—Br], 1.67 [m, 2H, CH$_2$—C—O], 1.5–1.2 [m, 8H, C—(CH$_2$)$_4$—C].

Quaternization of the Pyridine Derivatives by M-C*n*-Br. An acetonitrile solution containing the alkyl bromide monomer [1 equiv, 0.2 mol·L^{-1}], the appropriate pyridine moiety (2 equiv of 4-methylpyridine, 4-cyanopyridine, 4-(dimethylamino)pyridine, and 4,4′-dipyridyl; 0.8 equiv of 4-tolylpyridine), a few milligrams of 3,5-dinitrobenzene (inhibitor), and NaI [1·10^{-2} equiv] was stirred for 2 days at 55–70 °C under nitrogen atmosphere, then concentrated (~½ volume) by rotary evaporation, and finally precipitated in dry ethyl ether. The precipitate was thoroughly washed with ether to remove all unreacted pyridine. The purified monomer was recovered by filtration and dried in vacuo at 40 °C overnight. Melting points are given in Table 2.

(16-Methacryloyloxyhexadecyl)4-methylpyridinium Bromide (M-C16-MP). Yield: 80% in the form of a white powder. Anal. Calcd for $C_{26}H_{44}NO_2Br$, 0.22 H_2O: C, 64.59; H,

9.26; N, 2.90; O, 7.35; Br, 16.53. Found: C, 64.06; H, 9.20; N, 2.83; O, 7.02; Br, 16.93. ^{1}H NMR (200 MHz, CDCl$_3$): δ = 9.26 [d, 2H, pyridinium in α position], 7.85 [d, 2H, pyridinium in β position], 6.09 [s, 1H, CH=C—COO cis], 5.53 [s, 1H, CH=C—COO trans], 4.92 [t, 2H, CH$_2$—N$^+$], 4.12 [t, 2H, CH$_2$—O], 2.67 [s, 3H, C—CH$_3$], 1.99 [m, 2H, CH$_2$—C—N$^+$], 1.93 [s, 3H, C=C(CH$_3$)], 1.69 [m, 2H, CH$_2$—C—O], 1.5–1.1 [m, 24H, C—(CH$_2$)$_{12}$—C].

(12-Methacryloyloxydodecyl)4-methylpyridinium Bromide (M-C12-MP).[26] Yield: 76% in the form of a pink powder. Anal. Calcd for $C_{22}H_{36}NO_2Br$, 0.10 H_2O: C, 61.70; H, 8.52; N, 3.27; O, 7.85; Br, 18.66. Found: C, 61.14; H, 8.45; N, 3.29; O, 7.92; Br, 19.13. ^{1}H NMR (200 MHz, CDCl$_3$): δ = 9.30 [d, 2H, pyridinium in α position], 7.88 [d, 2H, pyridinium in β position], 6.07 [s, 1H, CH=C—COO cis], 5.52 [s, 1H, CH=C—COO trans], 4.88 [t, 2H, CH$_2$—N$^+$], 4.10 [t, 2H, CH$_2$—O], 2.65 [s, 3H, C—CH$_3$], 1.95 [m, 2H, CH$_2$—C—N$^+$], 1.91 [s, 3H, C=C(CH$_3$)], 1.64 [m, 2H, CH$_2$—C—O], 1.5–1.1 [m, 16H, C—(CH$_2$)$_8$—C].

(8-Methacryloyloxyoctyl)4-methylpyridinium Bromide (M-C8-MP). Yield: 68% in the form of a red waxy material. ^{1}H NMR (300 MHz, CDCl$_3$): δ = 9.28 [d, 2H, pyridinium in α position], 7.84 [d, 2H, pyridinium in β position], 6.10 [s, 1H, CH=C—COO cis], 5.56 [s, 1H, CH=C—COO trans], 4.88 [t, 2H, CH$_2$—N$^+$], 4.12 [t, 2H, CH$_2$—O], 2.68 [s, 3H, C—CH$_3$], 1.95 [s, 3H, C=C(CH$_3$)], 2.02 [m, 2H, CH$_2$—C—N$^+$], 1.65 [m, 2H, CH$_2$—C—O], 1.5–1.2 [m, 8H, C—(CH$_2$)$_4$—C].

(12-Methacryloyloxydodecyl)4-cyanopyridinium Bromide (M-C12—CP). Yield: 62% in the form of a yellow powder. Anal. Calcd for $C_{22}H_{33}N_2O_2Br$, 0.08 H_2O: C, 60.21; H, 7.61; N, 6.38; O, 7.58; Br, 18.21. Found: C, 59.80; H, 7.63; N, 6.40; O, 7.50; Br, 18.69. ^{1}H NMR (200 MHz, CDCl$_3$): δ = 9.82 [d, 2H, pyridinium in α position], 8.45 [d, 2H, pyridinium in β position], 6.09 [s, 1H, CH=C—COO cis], 5.52 [s, 1H, CH=C—COO trans], 4.13 [t, 2H, CH$_2$—O], 2.06 [m, 2H, CH$_2$—C—N$^+$], 1.94 [s, 3H, C=C(CH$_3$)], 1.66 [m, 2H, CH$_2$—C—O], 1.5–1.1 [m, 16H, C—(CH$_2$)$_8$—C].

(12-Methacryloyloxydodecyl)4-dimethylaminopyridinium Bromide (M—C12-DMAP). Yield: 82% in the form of a white powder. Anal. Calcd for $C_{23}H_{39}NO_2Br$, 0.64 H_2O: C, 59.15; H, 8.69; N, 6.00; O, 9.04; Br, 17.11. Found: C, 58.72; H, 8.62; N, 6.01; O, 8.64, Br, 17.63. ^{1}H NMR (200 MHz, CDCl$_3$): δ = 8.46 [d, 2H, pyridinium in α position], 7.03 [d, 2H, pyridinium in β position], 6.08 [s, 1H, CH=C—COO cis], 5.53 [s, 1H, CH=C—COO trans], 4.33 [t, 2H, CH$_2$—N$^+$], 4.11 [t, 2H, CH$_2$—O], 3.26 [s, 6H, (CH$_3$)$_2$—N], 1.93 [s, 3H, C=C(CH$_3$)], 1.82 [m, 2H, CH$_2$—C—N$^+$], 1.65 [m, 2H, CH$_2$—C—O], 1.5–1.1 [m, 16H, C—(CH$_2$)$_8$—C].

(12-Methacryloyloxydodecyl)4-(4′-tolyl)pyridinium Bromide (M-C12-TP). Yield: 64% in the form of yellow crystals. Anal. Calcd for $C_{28}H_{40}NO_2Br$, 0.5 H_2O: C, 65.74; H, 7.88; N, 2.74. Found: C, 65.47; H, 8.11; N, 2.80. ^{1}H NMR (300 MHz, CDCl$_3$): δ = 9.37 [d, 2H, pyridinium in α position], 8.18 [d, 2H, pyridinium in β position], 7.69 [d, 2H, tolyl in 2′,6′ position], 7.39 [d, 2H, tolyl in 3′,5′ position], 6.10 [s, 1H, CH=C—COO cis], 5.55 [s, 1H, CH=C—COO trans], 4.94 [t, 2H, CH$_2$—N$^+$], 4.13 [t, 2H, CH$_2$—O], 2.47 [s, 3H, tolyl-CH$_3$], 2.05 [m, 2H, CH$_2$—C—N$^+$], 1.95 [s, 3H, C=C(CH$_3$)], 1.65 [m, 2H, CH$_2$—C—O], 1.5–1.1 [m, 16H, C—(CH$_2$)$_8$—C].

(12-Methacryloyloxydodecyl)4-(4′-pyridyl)pyridinium Bromide (M-C12-PP). The crude product stemming from the quaternization by 4,4′-dipyridyl[24,25] was purified by column chromatography [eluent: chloroform/methanol (⁷/₃ v/v)]. NMR, TLC and ESMS [electrospray mass spectrometry, performed using a SCIEX API III triple quadruple mass spectrometer (Mass Spectrometry Lab, Toronto, Canada)] indicated the complete removal of 4,4′-dipyridyl and 12-methacryloyloxydodecyl-4,4′-bipyridinium dibromide. Yield: 57% in the form of yellow crystals. Anal. Calcd for $C_{26}H_{37}N_2O_2Br$, 2.5 H_2O: C, 58.42; H, 7.92; N, 5.24. Found: C, 58.11; H, 7.52; N, 5.36. ^{1}H NMR (300 MHz, CD$_3$OD): δ = 9.16 [d, 2H, pyridinium in α position], 8.83 [d, 2H, pyridinium in β position], 8.53 [d, 2H, pyridine in 3′,5′ position], 8.02 [d, 2H, pyridine in 2′,6′ position], 6.06 [s, 1H, CH=C—COO cis], 5.60 [s, 1H, CH=C—COO trans], 4.71 [t, 2H, CH$_2$—N$^+$], 4.12 [t, 2H,

Table 3. Free-Radical Polymerization Characteristics of the Quaternized Monomers

run	monomer	[M] (mol·L^{-1})	[I]/[M] ($\times 10^{-2}$)	yield (%)
1	M-C16-MP[a]	0.2	1.0	97
2	M-C12-MP[a]	1.0	1.0	55
3	M-C12-MP[a]	0.2	1.0	43
4	M-C8-MP[a]	0.9	0.5	71
5	M-C12-CP[a]	0.2	1.0	60
6	M-C12-DMAP[b,c]	0.9	0.5	<10
7	M-C12-DMAP[b,d]	0.2	1.0	95
8	M-C12-TP[d–f]	0.2	1.0	55
9	M-C12-PP[d–f]	0.2	1.0	18

[a] Homogeneous solution at $t = 0$, gelled at the end of polymerization. [b] Gel free. [c] Polymerized in ethanol. [d] Turbid solution throughout the polymerization reaction. [e] Polymerized at 70 °C. [f] Heterogeneous solution at $t = 0$, gelled at the end of polymerization. Abbreviations: [M], monomer concentration; [I], initiator concentration.

Scheme 1
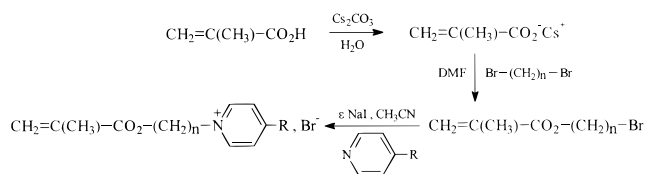
CH$_2$-O], 2.08 [m, 2H, CH$_2$- C-N$^+$], 1.93 [s, 3H, C=C(CH$_3$)], 1.66 [m, 2H, CH$_2$-C-O], 1.55–1.2 [m, 16H, C-(CH$_2$)$_8$-C]. ESMS: $m/z =$ (M − Br$^-$)$^+$ = 409.6.

Polymerization. Following several freeze−thaw cycles to degas the solutions, the quaternized monomers were all polymerized free radically in aqueous micellar conditions for 15−20 h at 60 °C (70 °C for M-C12-PP and M-C12-TP), using the sodium salt of ACVA as initiator. Monomer and initiator concentrations and other details related to the polymerizations are given in Table 3. In all cases except M-C12-DMAP (turbid solution throughout the reaction), the polymer formed a gel by the end of the reaction. All polymers, except PM-C12-DMAP [which was precipitated in a mixture of acetone/ether (80/20 v/v)], were purified by exhaustive dialysis for 4−7 days according to two different procedures depending on the solubility of the polymer, using Spectrapor membranes (VWR) with a molecular weight cutoff of 3500: (a) in pure water for PM-Cn-MP[26] and PM-C12-CP; (b) initially in aqueous ethanol (∼50/50 v/v) progressively enriched in ethanol and terminating in pure ethanol for PM-C12-TP and PM-C12-PP. All polymers were recovered by freeze-dying, except for PM-C12-TP and PM-C12-PP, which were dried in vacuo directly after the removal of ethanol by rotary evaporation. The lack of residual monomer was verified on representative samples by (a) ^{1}H NMR (CD$_3$-OD) for PM-C12-DMAP, which shows the complete disappearance of the α-CH$_3$ singlet of the unsaturated methacrylate moiety at ∼1.9 ppm, and (b) by FTIR for PM-C12-MP and PM-C16-MP, showing no evidence of the monomer band[27] at 940 cm^{-1} (CH out-of-plane deformation of the double bond).

Results and Discussion

Synthesis of the Monomers. The general strategy for the synthesis of the monomers is shown in Scheme 1, and involves two main steps which will be discussed successively.

The first step entails an SN$_2$ substitution between a methacrylate salt and the appropriate α,ω-dibromo-alkane taken in excess to give the alkyl bromide monomer. According to the literature,[22] this process is most efficient when performed in a homogeneous DMF solution with Cs$^+$ as the counterion. Furthermore, an issue of major importance is the correlation between the yield of the target monomethacrylate and the initial stoichiometric ratio, $r =$ [methacrylate]$_0$/[α,ω-dibromo-

Table 4. Calculated and Experimental Yields, τ, of the Alkyl Bromide Methacrylate Monomers

monomer	r^a	τ/% calcd	τ/% exptl
M-C8-Br	0.50	75	77
M-C12-Br	0.34	83	80
M-C16-Br	0.50 (first experiment)	75	79
	0.50 (second experiment)	75	72

[a] r: [cesium methacrylate]$_0$/[α,ω-dibromoalkane]$_0$.

alkane]$_0$. Assuming that the two reaction sites behave independently, the mole fractions of the unreacted α,ω-dibromoalkane, the monosubstituted derivative, and the disubstituted derivative—P_0, P_1, and P_2, respectively—are given by

$$P_0 = (1 - p)^2 \tag{2}$$

$$P_1 = 2p(1 - p) \tag{3}$$

$$P_2 = p^2 \tag{4}$$

where p is the probability of reaction of one brominated site. The yield, τ, of the target monomer calculated with respect to cesium methacrylate is then given by

$$\tau = P_1/(P_1 + 2P_2) \times 100 = (1 - p) \times 100 \tag{5}$$

where, if the reaction is quantitative with respect to the salt, p is given by

$$p = r/2 \tag{6}$$

The good agreement between the experimental and calculated τ values—as shown in Table 4 for the three alkyl chain lengths, n, and two stoichiometric ratios, r—implies that the salt is totally consumed during the reaction and shows that the two reaction sites of Br−(CH$_2$)$_n$−Br are independent, as would be expected from the high n values.[28] It should be noted that the use of a higher excess of α,ω-dibromoalkane than used experimentally would result in only a small improvement in the reaction yield at the expense of the purification process (involving removal of a large amount of unreacted reagent, all the more undesirable in the case of the expensive C16 dibromide).

The second step entails the quaternization of the desired pyridine derivative by the alkyl bromide monomer in acetonitrile in the presence of a catalytic amount of NaI. The quaternization yield is greater than 60% for the monopyridines, with the lowest yield obtained for the 4-cyanopyridine whose lesser reactivity can be attributed to the strong electronegativity of the cyano substituent. For 4,4′-bipyridine, it is 57%, compared to a theoretical yield of 75% ($r =$ [monomer]/[4,4′-bipyridine] = 0.5).

General Characteristics of the Monomers. Most of the quaternized monomers are colored species (ranging from yellow to red; see the Experimental Section), as is often observed for 4-substituted pyridinium halides,[19,20,29] which is ascribed to an intramolecular charge-transfer complex between the halide and the pyridinium ring.[29]

All monomers are easily soluble at ambient temperature in the usual alcohols, such as ethanol and methanol, as well as in the weakly polar and protic solvent, chloroform. They are also soluble in water, more easily for the monomers with short aromatic moieties

(Y = CP and MP) than for those with the more elongated aromatic moieties (Y = PP and TP), which is ascribed to the greater hydrophobic character of the latter. On the other hand, aqueous solutions of the monomers at the concentrations used for polymerization (higher than 0.1 mol·L^{-1}; see Table 3) are probably of the micellar type, as suggested by the cmc value of about 0.015 mol·L^{-1} measured[30] at 25 °C for a very similar monomer (11-methacryloyloxy-undecylpyridinium bromide).

Because of their ionic character, the monomers are fairly hygroscopic, as reflected by their elemental analysis (see the Experimental Section), and they are difficult to obtain in an anhydrous form, since possible thermal polymerization precludes drying them at sufficiently high temperatures. Despite these problems, some trends in their thermal properties, as listed in Table 2, are apparent. First, the melting point is significantly lower, the shorter the alkyl tail (compare M-C8-MP, a paste at room temperature, with M-C12-MP, which melts at 60 °C). Second, the mesogens with the more elongated aromatic group, notably M-C12-TP and M-C12-PP, have a much higher melting point than those with the shorter aromatic group, notably M-C12-MP and M-C12-DMAP. Although a contribution from incomplete drying cannot be ruled out, these trends are reasonable.

Of the monomers for which DSC thermograms were obtained (*n* = 12 only), a single transition, with a high enthalpy (40−60 J/g) typical of a transition between a crystalline phase and a disordered phase, is observed for M-C12-MP and M-C12-TP only. This is consistent with results from a previous publication,[21] where a disordered smectic A phase appears in low molar mass alkylpyridinium mesogens of the MP and TP type for very long alkyl chains (*n* ≥ 16) only. Polarizing optical microscopy observations show that these samples melt directly into the isotropic phase. M-C12-PP, on the other hand, melts into a disordered mesophase at 96 °C and becomes isotropic at 117 °C (enthalpy, Δ*H*: 1 J/g). M-C12-CP and M-C12-DMAP display a more complex thermotropism. M-C12-CP has a major transition (Δ*H*: 70−90 J/g) at 58 or 71 °C, depending on the sample history, and two additional transitions of similar enthalpies (Δ*H*: 10 J/g) at 87 °C (where it becomes transparent in nonpolarized light) and 102 °C, after which the isotropic state is attained. The two mesophases appear to be relatively ordered according to POM observations (limited mobility and lancelike textures on cooling from the isotropic phase); however, this could not be confirmed by X-ray scattering analysis, and limited sample precluded further study. Similarly, M-C12-DMAP shows a major transition in the first scan at 55 or 62 °C, depending on sample history, which does not reappear on subsequent scans after cooling from the isotropic phase, as well as a second and reversible transition to the isotropic phase at 82 °C (Δ*H*: 35 J/g) and from the isotropic phase near 62 °C (Δ*H*: 30 J/g). Again, we were unable to determine the precise nature of the mesophase, but the enthalpies and POM observations suggest a highly ordered phase. Thus, of all the monomers prepared, only PP and possibly CP and DMAP appear to be thermotropic liquid crystals.

Polymerization and Polymer Solubility. A preliminary attempt to perform free radical polymerization of M-C12-DMAP in a homogeneous ethanol solution at 60 °C, using AIBN as initiator, resulted in a very poor yield of less than 10% (run 6 in Table 3), in agreement with literature data on similar systems.[31] Polymeriza-

tions were therefore performed in aqueous micellar solutions (monomer concentrations in the range 0.2−1 mol·L^{-1}), using the sodium salt of ACVA as initiator; this gave medium to nearly quantitative yields (Table 3).

Gelation of the reactive medium at the end of aqueous polymerization was systematically observed except for PM-C12-DMAP (run 7 in Table 3). Considering that polymerization in micellar conditions often leads to high molecular weight,[32,33] which may contribute to gelation, we added various amounts of 2-mercaptoethanol (ME), an efficient transfer agent [C_T(60 °C) = 0.62 for methyl methacrylate[34]], to the monomer, M-C12-MP, under otherwise identical polymerization conditions. It was observed that, for ratios[35] of [ME]/[M-C12-MP] greater than about 1×10^{-2}, gelation following polymerization is inhibited. Thus, the gelation may tentatively be ascribed to a physical network, involving strong hydrophobic interactions among very long amphiphilic chains, that develops in the aqueous medium over a rather broad concentration range (2−25 g·dL^{-1}). The presence of lyotropic mesophases is also not ruled out.

Once isolated and dried, the polymers were essentially insoluble in the various solvents tested: (a) water and protic solvents such as alcohols (methanol, ethanol, and trifluoroethanol), formamide and *N*-methylformamide; (b) dipolar aprotic solvents such as DMF and 1-methyl-2-pyrrolidinone; (c) binary solvents associating a weakly polar species with good solvation power for the apolar chain and a protic species capable of solvating the ionic moiety such as chloroform/methanol (this last category was tested only for PM-C12-MP). Only PM-C12-DMAP showed limited solubility in solvents of category a. On the other hand, we noted that exchanging the bromide counterion for a sulfonated surfactant counterion (e.g., a stoichiometric complex of PM-C12-MP and octyl sulfonate) does lead to materials which are soluble in water, alcohols, and formamide, albeit with more difficulty for polymers obtained in the presence of small amounts of transfer agent or no transfer agent.[36]

Two possible explanations for the insolubility can be proferred. First, the amphiphilic character combined with the effects of possibly very high molar mass may limit the polymer solubility; at least in water[31] and very polar solvents, the ionic groups may be tightly bound and buried in a hydrophobic network and thus inaccessible to solvation.[31] Laschewsky and co-workers[3,6,7] generally report greater solubility of tail-end polyamphiphiles in highly polar (protic) solvents than we observe; but they also noted that those involving an aromatic ring (pyridinio sulfonate)—and all of our polyamphiphiles involve an aromatic ring—are more restricted in solubility than those without aromaticity (tetraalkylammonio sulfonate), attributing this to additional strong interactions among the aromatic rings.[3] Second, we cannot entirely eliminate the possibility that very light cross-linking by undetectable amounts of α,ω-dimethacrylate left in the monomers may have occurred, despite the two purification steps involved in their synthesis (column chromatography for the precursor alkyl bromide and crystallization in diethyl ether for the pyridinium salt); if very light, this may manifest itself only for higher molar mass, and hence be occulted in polymers obtained in the presence of sufficient transfer agent. However, this does not explain the significantly greater solubilities of the surfactant-complexed polymers compared to the Br-neutralized polymers. What-
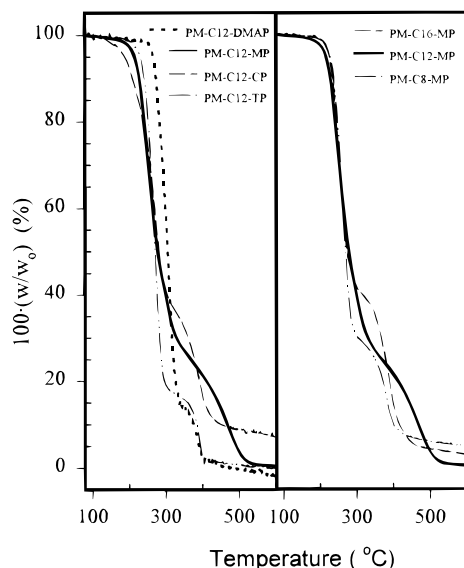
Figure 1. Thermogravimetric scans under nitrogen of PM-C*n*-Y polyamphiphiles.

ever the precise explanations, the only consequence of the lack of solubility is that it precludes molar mass determinations, which is a minor drawback for the purposes of this paper.

Finally, it is noted that, according to the literature,[37] radical polymerization of (11-methacryloyloxy)undecyltrimethylammonio bromide in aqueous solution at 25 °C yields a predominantly syndiotactic chain characterized by a probability of meso placement, P_m, of about 0.18. Our systems closely resemble this one, and we may therefore reasonably expect similar tacticities (with a slightly higher P_m due to somewhat higher polymerization temperatures).

Thermal Analysis. The thermal stability of the polymers was examined by thermogravimetric analysis. Figure 1 shows that thermal degradation occurs in two main steps, with the majority of the weight loss occurring in the first step. The temperature at which degradation begins (Table 4) depends on the nature of the mesogen. PM-C12-CP is the least stable, with weight loss beginning at approximately 130 °C and occurring somewhat more gradually (5% loss at 190 °C) than for the others. The most stable of the polymers measured is PM-C12-DMAP, for which degradation begins at about 230 °C (5% loss at 265 °C). The length of the spacer in the range studied plays a minor role in the stability, as shown by the PM-C*n*-MP series.

DSC traces for the various PM-C*n*-Y are shown in Figure 2. All polymers clearly display a glass transition (T_g), with a width of about 15–20 °C and a ΔC_p of about 0.3 J·g^{-1}·K^{-1}. Their temperatures are given in Table 5. None of the polymers except PM-C12-TP display other detectable transitions in the temperature range studied; the latter exhibits a weak endotherm ($\Delta H = 1.3$ J/g) at 157 °C (144 °C on cooling). It was also noted that the T_g's of all the PM-C12-MP samples polymerized in the presence of transfer agent are identical within experimental error (± 2 °C) to that of the same polymer polymerized without transfer agent, suggesting that the molar masses, in all cases, are above the range where they influence the T_g significantly.

It may be added that the first heating scans of the samples were generally different from the subsequent scans, frequently displaying significantly lower T_g's (ca.
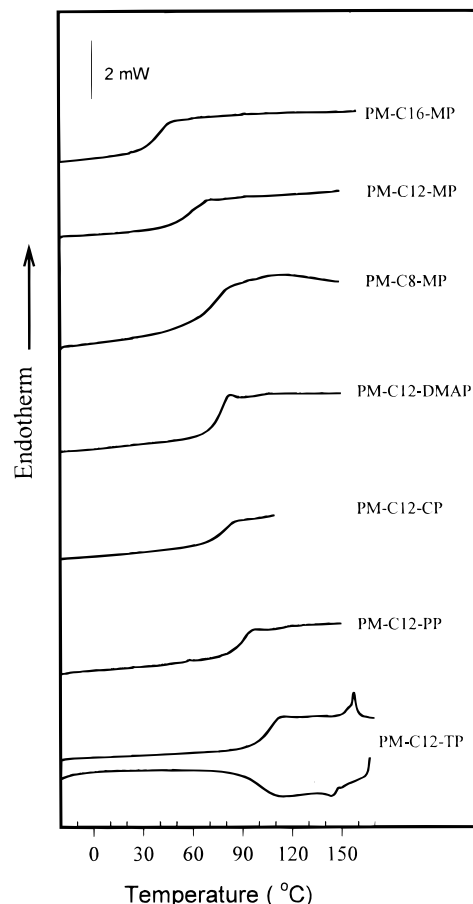

Figure 2. Representative DSC thermograms (heating scans) of the PM-C*n*-Y polyamphiphiles. A cooling scan of PM-C12-TP is also shown.

Table 5. Degradation Temperatures, T_d, and Glass Transition Temperatures, T_g, of the Polyamphiphiles

polymer	$T_d{}^a$/°C	T_g/°C
PM-C16-MP	225	39
PM-C12-MP	215	58
PM-C8-MP	230	86
PM-C12-CP	190	79
PM-C12-DMAP	265	76
PM-C12-TP	230	105
PM-C12-PP	b	89

[a] Measured at 5% weight loss relative to the dry weight at 80 °C. [b] Not measured.

10 °C), sometimes two apparent heat capacity jumps, much higher ΔC_p's, and, in some cases, enthalpic relaxations (PM-C12-DMAP and PM-C12-MP, in particular, showed distinct enthalpic relaxations after annealing times varying between 1 week and 3 months, respectively, at ambient temperature in a desiccator containing $CaCl_2$). Some or all of these phenomena, especially the decrease in T_g, may be related to the presence of H_2O. For example, it has been shown that annealing peaks that sometimes develop in ionomers under similar conditions as above (stored over $CaSO_4$ for long times) can be attributed to water absorption.[38] An endothermic peak attributed to the loss of bound water after storage in ambient (but not dry) atmosphere has been reported for other polyamphiphiles.[3]

Figure 3 shows that both the length of the alkyl spacer and the chemical nature of the mesogen strongly influence the T_g values. First, the T_g decreases in approximately linear fashion with increase in the
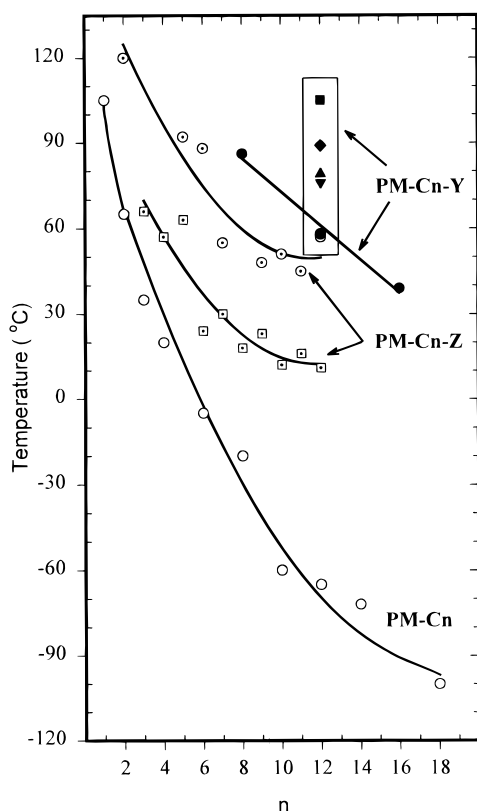
Figure 3. Glass transition temperature as a function of the number of carbons in the alkyl chain/spacer, *n*, of the PM-C*n*-Y polyamphiphiles of this study (MP, ●; DMAP, ▼; CP, ▲; PP, ◆; TP, ■), of poly(*n*-alkyl methacrylates)[39] (PM-C*n*, ○), and of nonionic mesogen-terminated alkyl polymethacrylates [PM-C*n*-Z with Z = −OΦΦCN[40] (⊡) and −OΦΦOCH₃[41] (⊙)]. The lines are guides to the eye.

number of carbons in the spacer (−6 °C/CH₂), illustrating a classic internal plasticization effect. The dependence of the T_g on spacer length is much stronger in our polymers than that reported for a series of poly[1-methyl-4-[2-[4-(((ω-methacryloyloxy)alkyl)oxy)phenyl]-vinyl]pyridinium tetraphenylborates] (*n* = 0, 6, 10),[12b] possibly because of the presence of the more bulky counterion in the latter. Second, the choice of pyridinium moiety results in T_g's ranging from 58 to 105 °C in the PM-C12-Y series, in the following order:

$$MP < CP \sim DMAP < PP < TP$$

It is noteworthy that the T_g of PM-C12-TP is identical to that generally reported for atactic poly(methyl methacrylate), thus indicating that the effect of the TP moiety on the T_g compensates for the plasticizing effect of the alkyl spacer.

It is useful to discuss these trends in comparison with other polymethacrylate polymers possessing a similar architecture, notably comblike polymers with simple *n*-alkyl side chains[39] and nonionic side-chain liquid crystal polymers (LCP's) possessing alkoxy biphenyl mesogens, one with a cyano tail[40] and one with a methoxy tail,[41] which are the closest nonionic analogues of our pyridinium mesogens for which relevant data are available. The T_g's for those polymers are also shown in Figure 3, thus highlighting the strong influence of the presence and nature of the mesogen, in addition to the side-chain length, on the T_g.

In all series, the T_g decreases with increasing alkyl chain/spacer length, as expected from the internal

plasticization effect; however, the rate of decrease varies significantly for the different series. It is most pronounced, not surprisingly, for the poly(*n*-alkyl methacrylates), where no mesogen is present. The T_g's of the nonionic side-chain liquid crystal polymers lie in a higher temperature range and decrease less rapidly overall than those of the *n*-alkyl polymers, tending toward a lower limiting value well before *n* = 12 (possibly, this latter is related to the presence of more ordered mesophases in many of these polymers). The higher temperature range of the T_g's can be associated with the rigidifying effect of the mesogen and to dipolar interactions among them.

Ionizing the mesogen clearly increases the temperature range of the T_g even further. This can be attributed, first of all, to the ionic interactions that are well-known to increase polymer T_g's.[18] However, an effect of mesogen rigidity on the T_g is clearly superposed on the effect of ionic interactions. Of the series studied (at constant spacer length, *n* = 12), the mesogen with the shortest aromatic moiety and a nonpolar tail, MP, possesses the lowest T_g. The addition of a second aromatic unit to the mesogen, giving TP, which significantly adds to its rigidity, increases the T_g by almost 50 °C. The somewhat lower value for PP, also possessing two aromatic units but not the methyl tail, indicates that the methyl tail plays a role in the effective rigidity. The higher T_g value of CP compared to MP can be related to strong dipolar interactions involving the cyano moiety. That of DMAP can be explained by its greater bulkiness and is perhaps also a result of charge delocalization over the methyl amino group, which requires that it be coplanar with the pyridinium ring, thus adding a rigidifying effect. It is also noted that, in the MP series, no lower limiting value seems evident for this series up to at least *n* = 16, in contrast to the nonionic LCP's.

Structural Analysis. All polymers display birefringence to varying extents when observed through the polarizing optical microscope, indicative of the existence of some structural order in the materials. The birefringence in the samples with short aromatic tails is fairly weak, white in color and ill-defined, although with a distinct gradation toward increasing intensity with increase in spacer length in the PM-C*n*-MP series. PM-C12-PP, and especially PM-C12-TP, display a more intense and colorful birefringence, although still ill-defined. Well-defined textures are difficult, if not impossible, to obtain, including after long annealing times, probably because of the high viscosity of the materials up to degradation temperatures (for example, although they yield quite easily to pressure at high temperatures, they remain very elastic). Upon heating, PM-C16-MP, PM-C12-CP, and PM-C12-TP remain birefringent up to their degradation temperatures, with PM-C12-TP becoming significantly less colorful near 160 °C (corresponding to the DSC endotherm). For PM-C12-DMAP, a decrease in birefringence begins near its T_g and is no longer observable at about 100 °C, and for PM-C8-MP, PM-C12-MP, and PM-C12-PP, birefringence is no longer observable at about 115, 130, and 150 °C, respectively; on cooling, it reappears beginning at about 115, 120, and 130 °C, respectively. Thus, the latter four samples apparently reach an effectively isotropic state, although the change is quite gradual (consistent with its being undetectable by DSC).
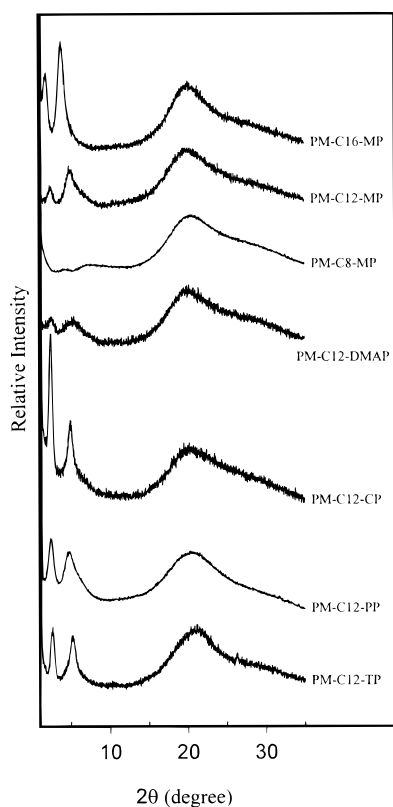
Figure 4. Ambient-temperature X-ray diffractograms of the PM-C*n*-Y polyamphiphiles.

Table 6. X-ray Scattering Data of the PM-C*n*-Y Polyamphiphiles at Ambient Temperature

polymer[a]	l_C/Å	d_1/Å	d_2/Å	d_w/Å
PM-C16-MP	32.3	47.0	23.0	4.4
PM-C16-MP[b]	32.3	42.0	21.7	4.4
PM-C12-MP	27.3	35.0	17.7	4.5
PM-C8-MP	22.3	20.8	~11.8	4.4
PM-C12-CP	27.7	36.5	17.9	4.4
PM-C12-CP[c]	27.7	34.5	17.4	4.4
PM-C12-DMAP	28.4	35.0	16.5	4.4
PM-C12-TP	31.1	34.0	17.0	4.2
PM-C12-PP	29.2	36.2	18.5	4.4

[a] Dried at 60 °C unless otherwise specified. [b] Dried in vacuo at 100 °C. [c] Dried in vacuo at 80 °C and then stored 3 days under P$_2$O$_5$. Abbreviations: l_C, calculated molecular length; d_1 and d_2, Bragg spacings determined from the first- and second-order diffraction peaks; d_w, Bragg spacing determined from the maximum of the wide angle halo.

To complement the POM observations, X-ray studies were undertaken. The X-ray profiles of the polymers under ambient conditions are shown in Figure 4, and associated data are given in Table 6. All are characterized by a broad halo centered at approximately 20° (2θ), corresponding to a Bragg distance of 4.4 Å, which can be taken to represent the average lateral spacing between disordered alkyl chains. The absence of diffraction peaks on the halo confirms that no crystalline order is present in these materials, in accordance with the DSC results. Similar results were obtained by Laschewsky and co-workers for their polyamphiphiles.[3–7] This is in contrast to *n*-alkyl comblike polymers that generally show crystallization beginning at shorter spacer lengths depending on the polymer backbone (at $n = 12$ for polymethacrylates),[42] as well as to nonionic side-chain LCP's that frequently display ordered and crystalline phases whose nature varies with spacer length.[43] It also contrasts with the low-molar-mass analogues previously studied, notably those with MP and TP moieties, which possess a crystalline or ordered phase up to relatively high temperatures and display a disordered lamellar phase (smectic A) only for alkyl chain lengths of 16 carbons or greater;[21] their conversion to polymeric form evidently interferes with crystallization, including for very long spacer lengths ($n = 16$).

At smaller angles, two reflections are consistently observed in all of the profiles. Their reciprocal spacings are in a 1:2 ratio (Table 6), which points to what is most likely a lamellar morphology (as frequently encountered in soaps and amphiphiles),[44] with the peak widths suggesting short correlation lengths. Their relative intensities and sharpness vary with aliphatic spacer length and the nature of the mesogenic moiety, probably reflecting differences in the definition, regularity and/or correlation lengths of the lamellar structures, with possible superposition of an intralamellar repeat distance; detailed analyses are under investigation and will be published separately.[45] Here, we will make some qualitative observations only. In the PM-C*n*-MP series, the first-order peak is less intense than the second-order peak (as also frequently observed by Laschewsky and co-workers);[3–6] furthermore, with decrease in spacer length, both peaks broaden and decrease in intensity relative to the wide-angle halo. A report[6] of a tail-end polyamphiphile with a hexyl (C6) spacer that produces no small-angle peaks is consistent with this tendency and with the fact that these peaks in our C8 polysoap are already very weak. The somewhat sharper and more intense peaks of PM-C12-TP and PP can be related to the more elongated mesogens favoring improved organization. The polymer with the bulkiest tail, PM-C12-DMAP, produces weak diffraction peaks, probably because the bulkiness hinders efficient packing, whereas the polymer with a very polar tail, PM-C12-CP, gives sharper and more intense peaks, especially the first-order one, which is consistent with the CN moiety generally stabilizing liquid crystalline phases (frequently in bilayers or partial bilayers)[44] and which is related to strong dipolar interactions leading to antiparallel mesogenic pairing.

The Bragg distances calculated from the small-angle reflections lie between one and two calculated side-chain lengths in most cases (Table 6). This suggests either orthogonal partial bilayers or tilted bilayers. In comparison, the smectic A phase of the low-molar-mass MP and TP analogues are monolayers.[21] Partial bilayer phases are, in fact, commonly found for polymeric versions of low molar mass mesogens that present monolayer phases, the presence of the polymer backbone presumably favoring an antiparallel arrangement of the mesogens with overlap of the mesogenic cores that may allow for optimal dipole−dipole interactions.[46] Accordingly, the superstructure of our polysoaps can be represented, to a first approximation subject to more detailed analyses,[45] by the general schematic shown in Figure 5, where the mesogenic groups are interdigitated and the alkyl spacers disordered to fill in the volume. Overall, the supramolecular structure of the ionic side-chain polyamphiphiles is similar to that of the (noncrystalline) *n*-alkyl side-chain polymers, which also tend to pack into layers albeit generally of a single side-chain thickness.[42]

The lack of greater order in the ionic polyamphiphiles may reflect joint interference to side-chain organization
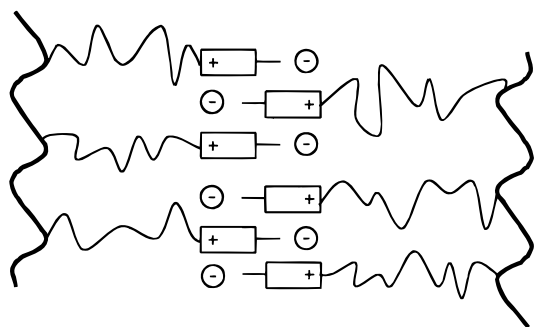
Figure 5. Simplified schematic of a possible supramolecular arrangement of the PM-C*n*-Y polyamphiphiles.

by attachment to the polymer backbone (as generally observed in side-chain polymer liquid crystals) *and* by ionic interactions at the tail end, having the effect that a significantly longer alkyl spacer is necessary to decouple ionic mesogens from the backbone. This is supported by the observation in the PM-C*n*-MP series that the shorter the alkyl spacer, the less well-defined the lamellar superstructure. Alternatively or additionally, the greater viscosity imparted to the melt by the ionic interactions may make potential transitions to greater order kinetically difficult, or the increase in T_g (compared to nonionic counterparts) as a result of the same ionic interactions may freeze in the disordered superstructure before further phase transitions can occur.

In additional experiments, diffraction profiles of several homopolymers were obtained at selected higher temperatures (limited due to the long exposure times necessary). In general, no dramatic changes were observed in the temperature range investigated (usually up to 120 °C). Only small shifts of the low-angle peaks to higher 2θ angles were noticed, an effect that is frequently observed for orthogonal lamellar morphologies and that is attributed to thermal motion creating greater disorder and resulting in a decrease in the lamellar thickness.[47] This shift is reversible, except for a proportion attributed to the loss of residual water molecules (see Experimental and Table 6). The already weak small-angle peaks for PM-C12-DMAP are still less distinct at 120 °C, which is consistent with the POM observations for this sample; however, their presence can still be detected. Similarly for PM-C12-MP, the first- and second-order peaks remain present, albeit less well-defined, up to at least 180 °C. It should also be mentioned that, for PM-C12-TP, no distinct morphological change could be detected by X-ray diffraction in the region of the DSC endotherm at 157 °C.

The continued presence of the first- and second-order small-angle X-ray peaks (although less well-defined) in the temperature range of apparent isotropism of some of the polymers, notably PM-C12-DMAP, combined with the slow disappearance of birefringence and no evidence of a corresponding DSC transition, may reflect a progressive decrease in size or correlation length of the lamellar regions to well below the wavelength of visible light (analogous to "cybotactic structures").[48] A similar explanation was given for the absence of birefringence between crossed polarizers, despite the presence of small-angle X-ray peaks indicating lamellar ordering, in complexes of poly(α,L-glutamate) and trimethyl-ammonium alkyl surfactants.[49]

Finally, it may be mentioned that there appears to be no particular relationship between the T_g value

obtained and the details of mesomorphic ordering. For example, although PM-C12-DMAP possesses the most poorly organized lamellar superstructure in the C12 series, its T_g is in the intermediate range and is very similar to that of PM-C12-CP, which, however, has a much better organized superstructure. This is not really surprising given that the morphology is influenced by packing considerations, whereas the T_g is affected primarily by the rigidity/flexibility of the pyridinium group and spacer. Therefore, whereas the bulkiness of the DMAP moiety can reduce the packing efficiency of the side chains, it may contribute to an increase in the T_g.

Conclusions

The above results show that the polymers studied tend to self-organize into a lamellar superstructure, similar to what has been observed for other ionic polyamphiphiles.[3−6] The driving force of this tendency is, no doubt, their amphiphilic character, consisting of incompatible highly polar hydrophilic and apolar hydrophobic parts, just as in low-molar-mass soaps and amphiphiles. However, in contrast to the latter, which tend to display a variety of thermotropic mesophases in the bulk,[50] the lamellar superstructure of the polyamphiphiles studied remains disordered in nature from high temperatures down to the glassy state, even for long spacers. Despite the overall similarity of the superstructures due to the amphiphilic nature of the polymers, it was observed that it is modulated in its definition by the spacer length and by the specific nature of the pyridinium group: increased spacer length improves the organization, as do more elongated mesogens and those characterized by specific, polar interactions, whereas bulky substituents are detrimental.

The amorphous nature of the superstructure, coupled with the plasticizing effect of the alkyl spacer, allows for the appearance of a well-defined glass transition at easily accessible temperatures. This, in turn, allows for an unambiguous analysis of the T_g's as a function of specific molecular parameters. In particular, the decrease in T_g with increase in alkyl spacer length appears to be linear in the range studied, $n = 8−16$, in contrast to what is found for analogous *n*-alkyl comblike polymers and nonionic side-chain liquid crystalline polymers. It was also observed that the T_g's of the polyamphiphiles are significantly greater than those of nonionic counterparts, a consequence of the ionic interactions among the pyridinium groups. However, this work also shows that, superposed on the effect of ionic interactions, is a strong modulating effect of the specific nature of the pyridinium moiety. This was related to differences in rigidity, as conferred by more elongated aromatic moieties, by greater bulkiness or by increased polar interactions. This study thus complements the sparse number of studies in the literature on ionic polyamphiphiles in the solid state, showing in particular the interplay between the effects of ionic interactions, spacer length, and specific structure of the ionic (pyridinium) group.

References and Notes

(1) Laschewsky, A. *Adv. Polym. Sci.* **1995**, *124*, 1.

(2) Anton, P.; Köberle, P.; Laschewsky, A. *Makromol. Chem.* **1993**, *194*, 1.

(3) Laschewsky, A.; Zerbe, I. *Polymer* **1991**, *32*, 2070.

(4) Köberle, P.; Laschewsky, A.; Tsukruk, V. *Makromol. Chem.* **1992**, *193*, 1815.

(5) Tsukruk, V.; Mischenko, N.; Köberle, P.; Laschewsky, A. *Makromol. Chem.* **1992**, *193*, 1829.

(6) Köberle, P.; Laschewsky, A. *Macromolecules* **1994**, *27*, 2165.

(7) Bonte, N.; Laschewsky, A. *Polymer* **1996**, *37*, 2011.

(8) Michas, J.; Paleos, C. M.; Dais, P. *Liq. Cryst.* **1989**, *5*, 1737.

(9) Lin, C.; Blumstein, A. *Am. Chem. Soc. Polym. Prepr.* **1992**, *33* (2), 118.

(10) Lin, C.; Feng, C. H.; Blumstein, A. *Am. Chem. Soc. Polym. Prepr.* **1993**, *34* (2), 737.

(11) Lin, C.; Cheng, P.; Blumstein, A. *Mol. Cryst. Liq. Cryst.* **1995**, *258*, 173.

(12) (a) Choi, D. H.; Kim, H. M.; Wijekoon, W. M. K. P.; Prasad, P. N. *Chem. Mater.* **1992**, *4*, 1253. (b) Choi, D. H.; Wijekoon, W. M. K. P.; Kim, H. M.; Prasad, P. N. *Chem. Mater.* **1994**, *6*, 234.

(13) Hessel, V.; Ringsdorf, H.; Festag, R.; Wendorff, J. H. *Macromol. Chem., Rapid Commun.* **1993**, *14*, 707.

(14) Chen, T. M.; Wang, Y. F.; Kitamura, M.; Nakaya, T.; Sakurai, I. *Macromolecules* **1995**, *28*, 7711.

(15) Navarro-Rodriguez, D.; Frère, Y.; Gramain, P. *Makromol. Chem.* **1991**, *192*, 2975; Navarro-Rodriguez, D.; Guillon, D.; Skoulios, A.; Frère, Y.; Gramain, Ph. *Makromol. Chem.* **1992**, *193*, 3117.

(16) Masson, P.; Gramain, Ph.; Guillon, D. *Macromol. Chem. Phys.* **1995**, *196*, 3677. Masson, P.; Heinrich, B.; Frère, Y.; Gramain, Ph. *Macromol. Chem. Phys.* **1994**, *195*, 1199. Ikker, A.; Frère, Y.; Masson, P.; Gramain, Ph. *Macromol. Chem. Phys.* **1994**, *195*, 3799.

(17) Ujiie, S.; Iimura, K. *Polym. J.* **1993**, *25*, 347; *Chem. Lett.* **1990**, 995.

(18) Eisenberg, A.; King, M. *Ion-Containing Polymers*; Academic Press: New York, 1977. Eisenberg, A.; Kim, J.-S. *Introduction to Ionomers*; John Wiley and Sons: New York, 1998.

(19) Bazuin, C. G.; Guillon, D.; Skoulios, A.; Nicoud, J. F. *Liq. Cryst.* **1986**, *1*, 181.

(20) Bazuin, C. G.; Guillon, D.; Skoulios, A.; Zana, R. *J. Phys.* **1986**, *47*, 927.

(21) Tabrizian, M.; Soldera, A.; Couturier, M.; Bazuin, C. G. *Liq. Cryst.* **1995**, *18*, 475.

(22) Wang, S. S.; Gisin, B. F.; Winter, D. P.; Makofske, R.; Kulesha, I. D.; Tzougraki, C.; Meienhofer, J. *J. Org. Chem.* **1977**, *42*, 1286. Kruizinga, W. H.; Strijtveen, B.; Kellogg, R. M. *J. Org. Chem.* **1981**, *46*, 4321. Dijkstra, G.; Kruizinga, W. H.; Kellogg, R. M. *J. Org. Chem.* **1987**, *52*, 4230.

(23) Lide, D. R., Ed. *Handbook of Chemistry and Physics*, 76th ed.; CRC Press: Boca Raton, FL, 1995.

(24) Anton, P.; Heinze, J.; Laschewsky, A. *Langmuir* **1993**, *9*, 77.

(25) Tundo, P.; Kippenberger, D. J.; Politi, M. J.; Klahn, P.; Fendler, J. H. *J. Am. Chem. Soc.* **1982**, *104*, 5352.

(26) A synthesis of the same monomer and corresponding polymer, but with $n = 11$, was reported recently in: Cochin, D.; Laschewsky, A.; Nallet, F. *Macromolecules* **1997**, *30*, 2278 (monomer). Koetse, M.; Laschewsky, A.; Mayer, B.; Rolland, O.; Wischerhoff, E. *Macromolecules* **1998**, *31*, 1, 9316 (polymer).

(27) Laschewsky, A.; Ringsdorf, H.; Schmidt, G.; Schneider, J. *J. Am. Chem. Soc.* **1987**, *109*, 788.

(28) Constantinides, I.; Lourdes-Guevra, M.; Macomber, R. S. *J. Org. Phys. Chem.* **1990**, *3*, 789. Constantinides, I.; Macomber, R. S. *J. Org. Phys. Chem.* **1992**, *5*, 327.

(29) Boucher, E. A.; Mollett, C. C. *J. Chem. Soc., Faraday Trans.* **1981**, *78*, 1401.

(30) Hamid, S. M.; Sherrington, D. C. *Polymer* **1987**, *28*, 325; *Br. Polym. J.* **1984**, *16*, 39.

(31) Hamid, S. M.; Sherrington, D. C. *Polymer* **1987**, *28*, 332.

(32) Paleos, C. M.; Malliaris, A. *J. Makromol. Sci., Rev. Macromol. Chem. Phys.* **1988**, *C28*, 404.

(33) Ohtani, N. Surface Active Monomers. In *Polymeric Materials Encyclopedia*; Salamone, J. C., Ed.; CRC Press: Boca Raton, FL, 1996; Vol. 10, p 8172.

(34) O'Brien, J. L.; Gornick, F. *J. Am. Chem. Soc.* **1955**, *77*, 4757.

(35) High ratios of [ME]/[M-C12-MP] were used to compensate for potential exclusion or depletion of ME at the sites of polymerization, namely within the micelles.

(36) Vuillaume, P.; Bazuin, C. G. To be published.

(37) Dais, P.; Paleos, C. M.; Nika, G.; Malliaris, A. *Makromol. Chem.* **1993**, *194*, 445.

(38) Goddard, R. J.; Grady, B. P.; Cooper, S. L. *Macromolecules* **1994**, *27*, 1710.

(39) Rogers, S. S.; Mandelkern, L. *J. Phys. Chem.* **1957**, *61*, 985. Hempel, E.; Beiner, M.; Renner, T.; Donth, E. *Acta Polym.* **1996,** *47*, 525. Floudas, G.; Stepanek, P. *Macromolecules* **1998**, *31*, 6951. Kine, B. B.; Novak, R. W. Acrylic and Methacrylic Acid Polymers. In *Encyclopedia of Polymer Science and Engineering*, 2nd ed.; Mark. H. F., Bikales, N. M., Overberger, C. G.;;, Menges, G., Eds.; Wiley-Interscience: New York, 1985; Vol. 1, p 211.

(40) Craig, A. A.; Imrie, C. T. *Macromolecules* **1995**, *28*, 3617.

(41) Craig, A. A.; Imrie, C. T. *J. Mater. Chem.* **1994**, *4*, 1705.

(42) Platé, N. A.; Shibaev, V. P. *J. Polym. Sci.: Macromol. Rev.* **1974**, *8*, 117.

(43) McArdle, C. B., Ed. *Side Chain Liquid Crystal Polymers*; Chapman and Hall: New York, 1989.

(44) Skoulios, A.; Guillon, D. *Mol. Cryst. Liq. Cryst.* **1988**, *165*, 317.

(45) Vuillaume, P.; Rawiso, M.; Bazuin, C. G. Work in progress.

(46) Keller, E. N. *Macromolecules* **1989**, *22*, 4597.

(47) Diele, S.; Brand, P.; Sackmann, H. *Mol. Cryst. Liq. Cryst.* **1972**, *16*, 105.

(48) De Vries, A. *J. Phys. Suppl. Fasc.* **1975**, *3*, C-1. De Vries, A. *Pramana* **1975**, *Suppl. 1*, 93.

(49) Ponomarenko, E. A.; Waddon, A. J.; Bakeev, K. N.; Tirrell, D. A.; MacKnight, W. J. *Macromolecules* **1996**, *29*, 4340.

(50) Skoulios, A. *Ann. Phys.* **1978**, *3*, 421.